crystals

MDPI

Review

Review: Electrochemiluminescence of Perovskite-Related Nanostructures

Volodymyr Vasylkovskyi [1,2], Iryna Bespalova [1,3,*], Mykola Slipchenko [1,3], Olena Slipchenko [2], Yuriy Zholudov [4] and Boris Chichkov [3]

[1] Institute for Scintillation Materials of the National Academy of Sciences of Ukraine, Nauky Ave. 60, 61072 Kharkiv, Ukraine
[2] Department of Metals and Semiconductors Physics, National Technical University «Kharkiv Polytechnic Institute», Kyrpychova Str. 2, 61002 Kharkiv, Ukraine
[3] Institute of Quantum Optics, Leibniz University Hannover, Welfengarten 1, 30167 Hannover, Germany
[4] Department of Biomedical Engineering, Kharkiv National University of Radio Electronics, Nauky Ave. 14, 61166 Kharkiv, Ukraine
* Correspondence: bespalova@iqo.uni-hannover.de

Abstract: Perovskite nanostructures are promising nanomaterials for their possible application in electrochemiluminescent (ECL) analytical systems due to their unique optical, electronic, and chemical properties. This review focuses on the most recent advances in the application of perovskite and perovskite-related nanostructures, with different chemical compositions and modifications, in ECL with various media, coreactants, and reaction types. The most optimal methods of perovskite nanoparticle synthesis and electrode modification methods were reviewed. Possibilities and perspectives of the use of perovskite-related nanostructures for the ECL generation were demonstrated.

Keywords: perovskite nanocrystals; electrochemiluminescence; electrode modification

Citation: Vasylkovskyi, V.; Bespalova, I.; Slipchenko, M.; Slipchenko, O.; Zholudov, Y.; Chichkov, B. Review: Electrochemiluminescence of Perovskite-Related Nanostructures. *Crystals* **2023**, *13*, 455. https://doi.org/10.3390/cryst13030455

Academic Editors: Shailesh Narain Sharma and Xiaoping Wang

Received: 8 February 2023
Revised: 21 February 2023
Accepted: 3 March 2023
Published: 5 March 2023

1. Introduction

Electrogenerated chemiluminescence or electrochemiluminescence (ECL) is a light-emission phenomenon in the course of electrochemical reactions [1]. This phenomenon is the basis of the ECL method of analysis of liquids, which finds numerous applications in biology, medicine, ecology, pharmacy, etc. [2,3]. Due to the electro-chemical character of light generation and control of reaction course by electrode potential, the ECL assay technique possesses unique sensitivity to analyte detection together with great potential for automation and miniaturization [4]. Optimization has a fundamental importance in the analysis of essential biological species. Current research efforts in the field of analytical application of the ECL are focused in several directions, including the search for new ECL active luminescent materials [3,5,6], new efficient coreactants, and ECL reaction schemes [7–9], new electrode structures and materials [10–13], and development of miniature analytical devices—ECL sensors [4,14,15].

Scientific research on applications of nanomaterials in the ECL field is motivated by the potential benefits of improving the sensitivity and stability of analytical systems and broadening the range of detectable agents [5,16,17]. A promising class of nanomaterials, perovskite and perovskite-related nanocrystals attract a lot of attention due to their strong luminescence and ability to tune their electronic and catalytic properties by varying the ratio of materials that form their crystal lattice. This mini-review discusses recent progress and prospects in research and applications of fluorescent perovskite nanomaterials in the ECL field.

The review contains summarized information on the types of perovskite nanocrystals (PeNCs) suitable for applications as new emitters in ECL systems and focused on types of available coreactants for anodic and cathodic ECL generation, and some peculiarities of

their use, feasible detection principles based on perovskite ECL systems and examples of their analytical applications.

2. Perovskite Nanomaterials

In recent years, a large number of ECL-emitting material species have been discovered, and their properties have been investigated. All these species are classified into organic, inorganic, and nanoparticle (NP) systems [1–3]. Among all fluorescent nanomaterials available today, we chose to focus on one of the most promising and cost-effective materials—perovskite nanocrystals (PeNCs) or so-called "perovskite-related structures". Perovskite nanomaterials attract great attention for their potential applications in such fields as: optoelectronics, energy storage, pollutants degradation, water splitting, and analytical chemistry [18,19].

Most research on ECL with PeNCs focuses on halide perovskites with 3D ABX_3 cubic structure, where A and B are monovalent and divalent cations, respectively, and X is a monovalent halide anion (Figure 1). The stability of the ABX3 structure of PeNCs is determined by the Goldschmidt tolerance factor (1) and octahedral factor (2):

$$t = \frac{r_a + r_x}{\sqrt{2}(r_b + r_x)} \quad (1)$$

$$\mu = \frac{r_b}{r_x} \quad (2)$$

where r_a, r_b, and r_x are the radii of the A, B, and X sites. For the stable state of the perovskite structure, the value of the Goldschmidt tolerance factor should be between 0.81 and 1.00, and the octahedral factor should not be outside the 0.44–0.9 range [20].

The newer Goldschmidt tolerance factor τ (3), presented by Christopher J. Bartel et. al., enables a better prediction of perovskite stability than the previous one because of another functional form. The 1D nature of τ allows the determination of perovskite probability as a continuous function of the radii and oxidation states of A, B, and X.

$$\tau = \frac{r_x}{r_b} - n_a\left(n_a - \frac{r_a/r_b}{\ln(r_a/r_b)}\right) \quad (3)$$

where n_a is the oxidation state of A, r_i is the ionic radius of ion i, $r_a > r_b$ by definition, and τ < 4.18 indicates perovskite [21].

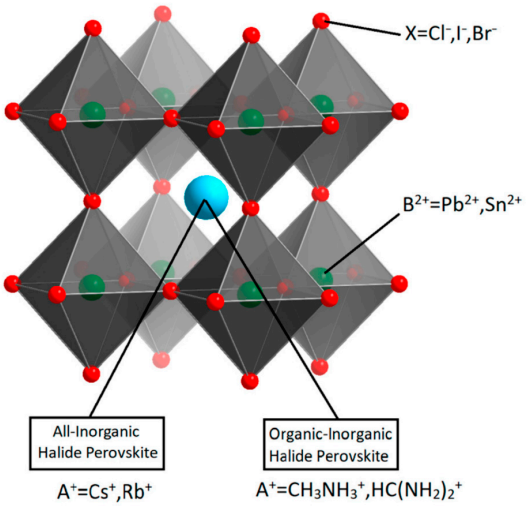

Figure 1. Schematic diagram of ABX_3 halide perovskite crystal structure. Reproduced from [22] © Permission according to Creative Commons Attribution License.

An important feature of this type of structure is that the optical and electronic properties of perovskite materials can be customized by varying the composition of constituted halide ions and to a smaller degree of the cations. In addition, the size and dimensionality of PeNCs can also be used to tune their optical properties [18]. The ability of simple reorganization of perovskite structure triggered the research of perovskite-related 0D and 2D structures such as: A_4BX_6 (0D); AB_2X_5 (2D); A_2BX_4 (2D); A_2BX_6 (0D); A_2BX_3 (2D); $A_3B_2X_9$ (2D); ABX_3 (3D); and $A_3B_3X_3$ (3D) [23]. There are not enough data to evaluate the influence of the nanocrystal dimension on the ECL signal, since the 0D and 2D structures were researched only once [24,25].

It is worth mentioning the application of doped PeNCs, namely, by manganese [26], cerium [27], and antimony [28]. Each dopant embeds into the cubic structure of PeNCs and, depending on the dopant, can enhance both absorbance and the electrochemical oxidation-induced hole-injection [27,28] and improve the stability of PeNCs [26]. However, such doping does not significantly change the electrochemical properties of PeNCs.

2.1. Synthesis of Perovskite Nanocrystals

The parameters to be considered during the synthesis of PeNCs from the viewpoint of their potential applications are: structure, stability, electronic, and optical properties [19]. By now, there has been significant progress in the shape-controlled methods of synthesis of PeNCs: Bulk to Nano, Heat up, Precipitation, and In situ synthesis [29]. However, only two methods of PeNCs synthesis for ECL applications have been frequently used: the hot injection technique [26–28,30,32–35] and the ligand-assisted reprecipitation technique (LARP technique) [25,36–40]. Using hot injection and the LARP technique, it is possible to synthesize highly luminescent PeNCs with fascinating optical properties which could be achieved by varying the ratio of initial precursors and start parameters of the synthesis procedure. Both methods are associated with the usage of precursors that are soluble or decomposable in solvents at low or high temperatures and producing monodisperse nanocrystals in "free" colloidal states which is important for the development of ECL sensors.

2.1.1. Ligand-Assisted Reprecipitation Technique

The LARP technique is a versatile, convenient, and low-cost approach for the synthesis of halide PeNCs. Reprecipitation through solvent mixing with the assistance of long-chain organic ligands is a simple way to prepare PeNCs. The formation of PeNCs can be performed within seconds by mixing the precursor solution consisting of a polar solvent, perovskite precursors, and organic ligand, with a nonpolar solvent under vigorous stirring at room temperature, without heating or a protective atmosphere (Figure 2). The LARP technique is based on a large difference in the precursor such as cesium halides CsX or organic molecule, in particular, methylammonium halides (MAX) and formamidinium halides (FAX) and PbX_2 (X = Cl, Br, I) solubility in their "good" (for example, dimethylformamide, ethyl acetate, or γ-butyrolactone) and "bad" (for example, toluene, chloroform, or acetone) solvents, wherein a "bad" solvent induces supersaturation and thus triggers the nucleation and further growth of PeNCs in presence of oleic acid and amine ligands. Therein, amine ligands such as n-octylamine or octadecylamine control the kinetics of crystallization and mainly contribute to the size control of PeNCs formed, whereas oleic acid suppresses aggregation effects and ensures their colloidal stability. The LARP technique is producing monodisperse nanocrystals mainly in the form of cubes with an edge length of 5–35 nm (depending on reaction conditions) in "free" colloidal states [21,25,36–44].

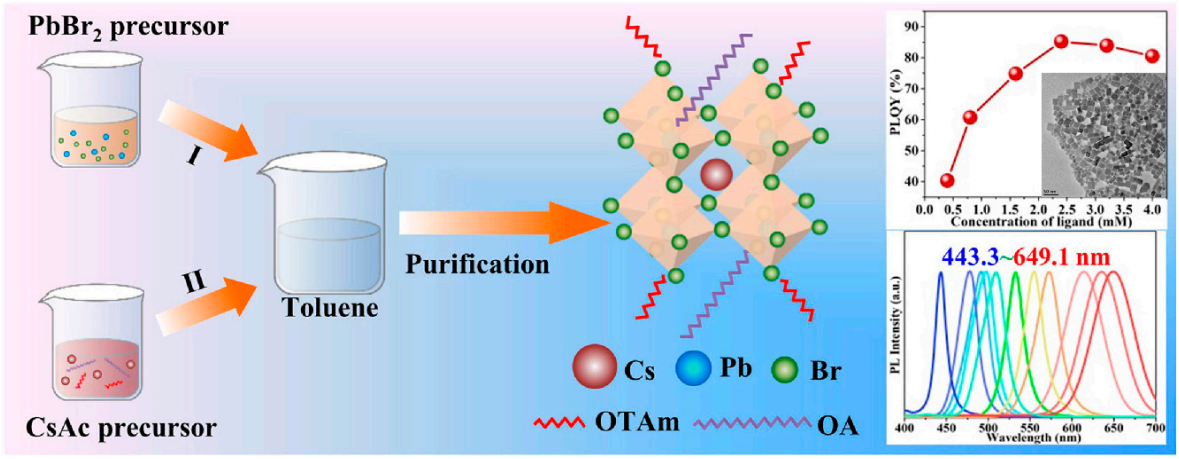

Figure 2. Synthesis of Colloidal $CsPbBr_3$ PeNCs via LARP method (Graphical abstract) [42]. © Elsevier.

2.1.2. Hot Injection Technique

The well-known hot injection technique also is applied for obtaining a variety of all-inorganic and organic-inorganic PeNCs in "free" colloidal states [19,23,29,44]. This technique is based on the rapid injection of one of the precursors into a hot solution of the remaining precursors, ligands, and a high boiling solvent with the use of a nitrogen atmosphere. The key parameters that enable control of the size, size distribution, and shape of PeNCs synthesized by the hot injection technique are: the injection temperature of one of the precursors; the concentration of the precursors, and the ratio of the surfactants to the precursors; and the reaction time. A different morphology of PeNCs is also obtained by the hot injection technique (Figure 3). Immediately after the injection of the precursor, rapid nucleation occurs with the formation of small nuclei which continue growing, as a rule, without new nuclei forming, which leads to the formation of PeNCs, which are characterized by a narrow size distribution. The standard procedure for obtaining PeNCs is realized by injecting Cs-oleate into a hot solution (140–200 °C) of PbX_2 (X = Cl, Br, I) salts, which served both as the Pb^{2+} and X^- sources, in octadecene (ODE), oleic acid (OA) and primary amines such as oleylamine (OLA) [23].

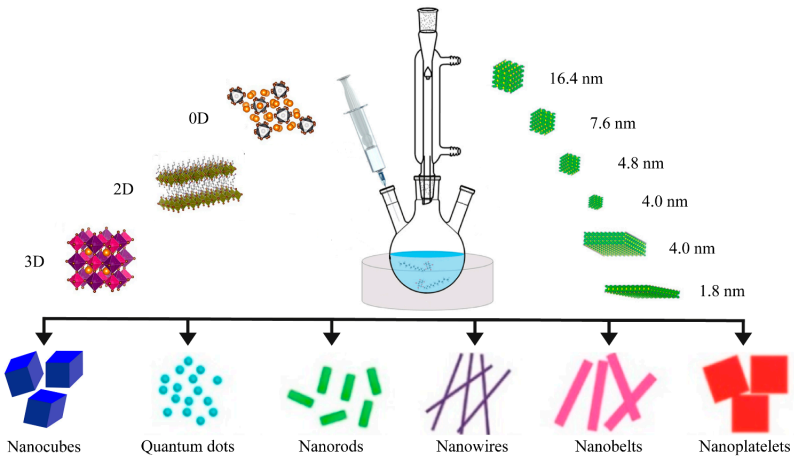

Figure 3. Scheme of the hot injection technique of colloidal synthesis. Reproduced from [23] © American Chemical Society.

So, the hot injection technique is producing different nanostructures of PeNCs with the sizes of 2–20 nm (by using, for example, OLA and OA as ligands), which mainly depend on the injection temperature and the ratio of the precursors (Figure 3).

2.1.2.1. Laser Ablation Synthesis of PeNCs

Both the hot injection technique and LARP synthesis utilize organic solvents and surface ligands; thus, both require additional complicated purification and isolation steps for obtaining pure PeNCs. The alternative way for the fabrication of nanomaterials in "free" colloidal state is based on pulsed laser ablation synthesis (PLA), which is a unique way of generating NPs from a variety of solid materials using a top-down physical approach and can be carried out in liquid, gaseous media, or in vacuum [45].

During the PLA process, the focused laser beam, targeted on a small region of solid material, ejects atomic, ionic, and nanoparticle species from the surface in the form of a plasma plume and material debris. The plume expands and cools down on a nanosecond time scale, which results in condensation, nucleation, and clustering with the formation of NPs [46]. The advantages of the PLA technique are the ultra-purity of obtained nanomaterials as well as the possibility to achieve stable colloids due to the in situ dispersion of NPs in a variety of liquids [47]. Such a method could be used for the fabrication of PeNCs as well.

Kanaujia et al. demonstrated the possibility of direct femtosecond laser ablation (λ = 410 nm, P = 100 mW) of 2D inorganic-organic cyclohexenyl ethyl ammonium lead iodide ($(C_6H_9C_2H_4NH_3)_2PbI_4$) films (thickness $\approx$ 135 nm) where perovskite micro- and NPs have been obtained as a by-product of laser writing (Figure 4). During the laser-material interaction, once the thin film melted, the material ejection occurred and formed a plasma plume that consisted of perovskite nano- and microparticles, which condensed at the nearby surface due to the temperature gradients and gravitational pull. The diameter of the obtained particles varied from 500 nm to 1 micron in size [48].

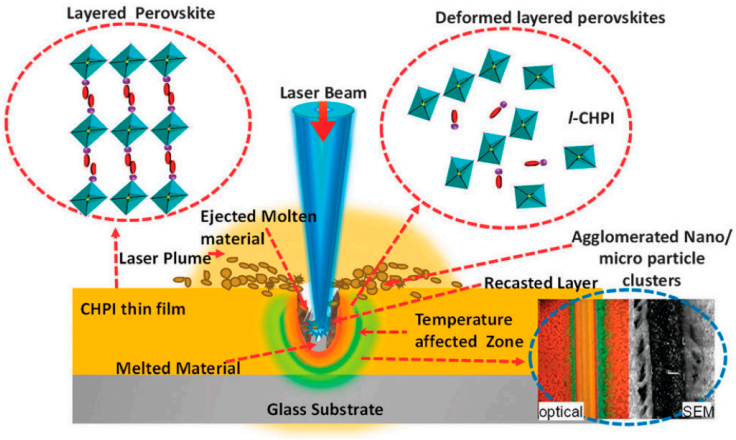

Figure 4. Schematic of the laser-material interaction during perovskite laser micropatterning and PeNCs formation. Reproduced with permission from [48]. © Royal Society of Chemistry.

The use of the pulsed laser ablation method may be promising for obtaining "pure" PeNCs free from chemical precursors and will not require a particle purification procedure. It can provide more opportunities for modifying the PeNCs surface and give higher flexibility for PeNCs incorporation into thin films for the modification of working electrodes for the ECL measurements.

3. Electrogenerated Chemiluminescence

Electrogenerated chemiluminescence is a powerful analytical technique combining the main advantages of electrochemical and chemiluminescent methods of the assay in terms of extremely high sensitivity and simple reaction control. As a result, the method finds its applications in numerous areas including immunoassay, water quality testing, food testing, biological agents' detection, etc. [3].

ECL is a phenomenon where light emission is produced in a solution near the electrode surface when a suitable potential is applied at the electrode. The ECL can occur in several ways, the most common are ion annihilation and coreactant ECL. In ion annihilation ECL,

the luminescent signal originates near the surface of the working electrode from the excited states of the luminophore. The latest is generated in a course of exo-energetic electron transfer reaction of electrochemically created radical ionic species. The scheme of the ion annihilation ECL reaction, which is the simplest case investigated at the beginning of the ECL era, is illustrated below, where *R* denotes a luminophore species [1]:

$$R - e \rightarrow R^{\bullet +} (\text{oxidation at the electrode}) \quad (4)$$

$$R + e \rightarrow R^{\bullet -} (\text{reduction at the electrode}) \quad (5)$$

$$R^{\bullet +} + R^{\bullet -} \rightarrow R + R^{*} (\text{excited state formation}) \quad (6)$$

$$R^{*} \rightarrow R + hv \ (\text{light emission}) \quad (7)$$

Such types of ion recombination reactions can work efficiently only in aprotic organic solvents and have little practical use for analytical science. In practical applications and for advanced ECL research, ion annihilation ECL is almost completely replaced nowadays by more complicated coreactant-type ECL. Coreactant ECL has the following advantages over ion annihilation ECL: it may produce a more intense ECL response when the annihilation reaction redox species are not efficient; the use of coreactant ECL can be possible for some fluorescent compounds that have only reversible EC oxidation or reduction; ability to achieve ECL signal in solvents with a narrow potential window such as aqueous solutions [49].

Corectants are chemical species that upon electrochemical reaction are consumed irreversibly due to the bond-breaking reaction to produce reactive by-products that can react with a reduced or oxidized luminophore and generate its excited state. Two possible ways of such reactions are called "oxidative reduction" of "reductive oxidation" [13]. The scheme below shows the mechanism of ECL with coreactant in the example of a reductive-oxidation reaction, where *C* represents the coreactant and P represents products associated with the Cox reaction [50].

$$\left.\begin{array}{l} R + e^{-} \rightarrow R^{-} \\ C + e^{-} \rightarrow C^{-} \end{array}\right\} (\text{reduction at the electrode}) \quad (8)$$

$$\left.\begin{array}{l} R^{-} + C \rightarrow R + C^{-} \\ C^{-} \rightarrow C_{ox} \\ C_{ox} + R \rightarrow R^{+} + P \end{array}\right\} (\text{homogenous chemical reactions}) \quad (9)$$

$$R^{-} + R^{+} \rightarrow R + R^{*} \text{ or } R^{-} + C_{ox} \rightarrow R^{*} + P \ (\text{excited state formation species}) \quad (10)$$

$$R^{*} \rightarrow R + hv (\text{light emission}) \quad (11)$$

4. Electrode Modification in Analytical ECL Applications

ECL assay can benefit from electrode modification with various functional structures and films that have great potential for the development of cheap, reliable, and reusable analytical ECL sensors. The use of various NPs of fluorescent and conductive materials for the functionalization of the electrode for electrochemical measurements is widely exploited to enhance their analytical performance [16,51].

Usually, as working electrode materials for ECL applications gold, indium tin oxide (ITO), graphite, or glassy carbon (GC) are used [11]. However, according to the reviewed publications, glassy carbon in the form of single-crystal appears to be the most suitable material for the ECL measurements as well as for the modification by NPs because of its suitable physical and chemical properties [25,26,30–34,36–40,52–58].

In the case of PeNCs ECL studies, their deposition on the electrode surface also plays a crucial role in enhancing NC stability in polar media, especially in aqueous solutions. There are two most common methods to obtain functional thin films with NPs for ECL measurements: drop-casting and spin-coating techniques. The drop-casting method (Figure 5a)

consists of two stages: deposition of the drop of a liquid solution containing a suspension of NPs and drying of the surface from the solvent [59]. The spin-coating technique includes the following stages: applying the solution with particles, rotating the electrode surface, and drying (Figure 5b) [60]. Despite the apparent similarity of these methods, the spin-coating method facilitates the production of uniform thin films, with the thickness of micro- and nanometers and uniform distribution of NPs over the surface of the electrode.

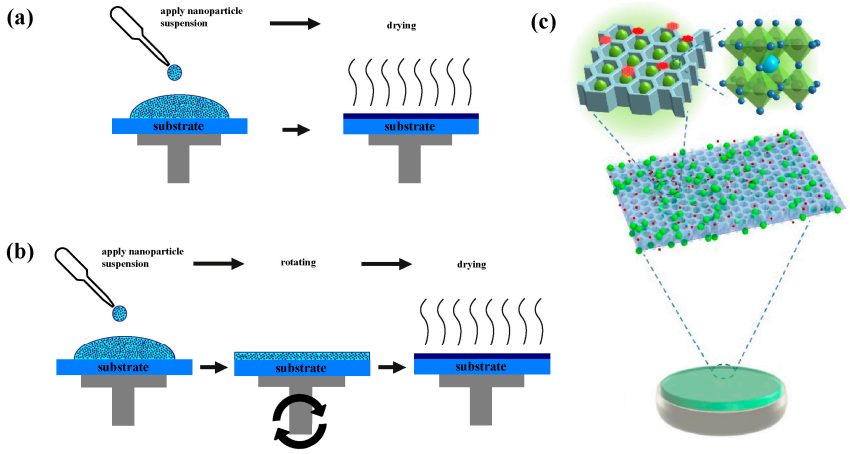

Figure 5. Schematic representation of electrode modification methods. (**a**) Drop-casting technique; (**b**) Spin-coating technique (Reproduced with permission from [61] © TechConnect) (**c**) Molecular imprinting technique [62] © Elsevier.

A molecularly imprinted polymer (MIP) (Figure 5c) is copolymerized by covalent or non-covalent binding between template molecules and functional monomers [35]. MIPs are used in molecular imprinting techniques for the ECL electrode modification as recognition elements. MIPs can be immobilized onto the surface of the working electrode via one-pot photopolymerization [62] or electropolymerization [35,63] with template molecules. MIPs improve the stability of PeNCs and provide high selectivity of the system. The disadvantage of MIP modification is the enhancement of electrical resistance of the modified electrode, which is caused by the charge transport blocking [62].

5. Media for the ECL Measurements with PeNCs

The choice of a supporting electrolyte solution has a great influence on ECL measurements with PeNCs since they can be negatively affected by polar solvents, heat, and oxygen because of its inherent ionic lead–halide bond and low formation energy of ligand binding [63]. The morphology and stability of perovskite thin films on electrodes under ECL conditions, including the applied potentials and selected electrolyte solution with appropriate polarity, are still issues yet to be studied [37]. In the reviewed ECL studies of PeNCs, reactions were achieved in aqueous and non-aqueous solutions.

5.1. ECL of Perovskite Nanocrystals in Non-Aqueous Solutions

For the investigation of new ECL systems, measurements are often conducted in oxygen-free cells with non-aqueous electrolyte solutions and special attention must be paid to solvents. That is because 3D all-inorganic cesium lead bromide PeNCs ($CsPbBr_3$) lose their luminescent properties in polar solvents including water. At the same time, water and oxygen can affect ECL reaction by quenching the formed excited state species by disabling the generation of reductive and oxidative precursors.

For the ECL with PeNCs, the following solvents were used in the observed articles: ethyl acetate (EA) [37], dichloromethane [24], acetonitrile [56], or acetonitrile/toluene mixture solution [25] (Figure 6). Some solvents can act not only as an electrolyte solution but as a coreactant. Ethyl acetate is a non-polar organic solvent that is used not only as an electrolyte solution but also as a coreactant for the ECL reaction with a potential

window between 0 and 1 V. Application of EA helped to achieve efficient ECL of $CsPbBr_3$ PeNCs [37].

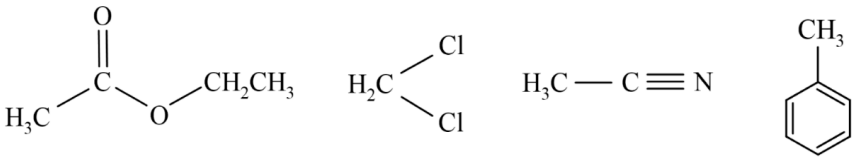

Ethyl acetate Dichloromethane Acetonitrile Toluene

Figure 6. Anhydrous solvents used for the ECL measurements with PeNCs.

Additionally, mixtures of solvents could be used for helping to dissolve certain compounds. Yue Cao et al. used the mixture of polar acetonitrile and non-polar toluene containing tetra-n-butylammonium hexafluorophosphate salt ($TBAPF_6$) where acetonitrile increased the dissolution of $TBAPF_6$, and toluene provided a suitable environment for the ECL reaction of 2D all-inorganic lead-free PeNCs ($Cs_3Bi_2Br_9$) with tripropylamine (TPrA) and benzoyl peroxide (BPO) as coreactants [25].

Despite less interest in non-aqueous buffer solutions from a practical point of view, such systems are suitable for studying the ECL of PeNCs because fewer factors can negatively affect ECL signal occurrence. Non-aqueous solutions are usually used for fundamental studies of ECL, i.e., for investigations of the possibility of obtaining ECL signal in new ECL systems.

5.2. ECL of Perovskite Nanocrystals in Aqueous Solutions

During cyclic voltammetry, which is a part of the ECL assay, redox reactions occur on the electrode surfaces. This process causes electrolysis that leads to a change in the pH of the aqueous solutions. Such an effect of electrolysis has to be neutralized, which is why supporting buffer electrolyte solutions are needed. The interest in ECL in aqueous solutions lies in the fact that the aqueous environment is natural for most of the bio-related detectable substances. The use of PeNCs in the ECL assay is an urgent task since PeNCs are highly hygroscopic in an aqueous or high-humidity environment due to their ionic crystal characteristics [52]. The reactivity of PeNCs toward moisture and their rapid dissolution in an aqueous environment severely limits both the study of their properties under the conditions that would degrade them and their applications.

The hydrophobization of PeNCs by the application of oleic acid (OA) and oleylamine (OLA) (or other compounds related to fatty acids) array networks is highly advantageous. That is to say, preventing the intrusion of polar solvents, allows ECL measurements to be performed in aqueous solutions [32]. OA and OLA facilitate superlattice formation through cross-linking of the long carbon chains by hydrophobic interaction, which prevented the intrusion of polar solvents and improved the stability of the PeNCs-containing film in an aqueous solution [31].

As an aqueous supporting electrolyte for the ECL measurements, a 0.1 M phosphate-buffered solution (PBS) is most often used [26,30–34,36,38,39,52,53,55,57,58]. PBS can be adapted to different pH levels from 5.8 to 7.4 and cannot be oxidized at low potentials up to a certain point. Such an aqueous solution is often used for the research of practical applications of ECL systems.

6. Coreactant ECL of PeNCs

All commercially available ECL setups are based on the coreactant ECL method. Unlike ion annihilation ECL, the solution for coreactant ECL must contain luminophore species and added reactant (coreactant). Typically, coreactant ECL is generated by applying an anodic or cathodic potential in a solution. Therefore, depending on the polarity of the applied potential, both luminophore and coreactant species can be oxidized or reduced at the electrode to form radical ions and intermediate species followed by the decomposition

of these species and the formation of excited states emitting light. Because highly reducing intermediate species are generated after the electrochemical oxidation of coreactant or highly oxidizing intermediates that are produced after electrochemical reduction, the corresponding ECL reactions are often defined as "oxidation-reduction" and "reductive-oxidation" ECL [50].

The types of PeNCs applicable for the generation of ECL with coreactants in both aqueous and non-aqueous media for the anodic and cathodic potential ranges are listed in Table 1. As seen from the table, despite difficulties connected with electroanalytical applications of PeNCs and the infancy of the PeNCs-related ECL research area, they appear to be rather versatile fluorescent nanostructures capable of efficient ECL emission with the variety of common coreactants that are currently used to implement different ECL assay procedures and formats. Among ECL coreactants that have already been studied with PeNCs are such well-known and widely utilized species as tertiary amine compound TPrA [27,28,32,40,55], peroxydisulfate anion [31,57], benzoyl peroxide [24,26,38], hydrogen peroxide [53], 2-dibutyaminoethanol [54], and prometryn [63]. Additionally, ECL of PeNCs was achieved with other amine compounds, such as diethanolamine, triethylamine, triethanolamine [32], 2,2′-(butylamine) diethanol, 3-(diethylamino) propylamine, [3-(diethylamino) propyl] trimethoxysilane [34], oleylamine present at the surface of PeNCs as stabilizing agent [36], as well as some other species such as ascorbic acid, which itself has analytical importance in biomedical assays [30,39], and ethyl acetate, which was used as a reaction medium [52,55].

Table 1. Application of perovskite nanocrystals in coreactant ECL.

Type of Nanoparticles	Solution	Coreactant	References
CsPbBr3 (3D)	Phosphate-buffered solution	Ascorbic acid;	[30]
		Potassium peroxydisulfate;	[31]
		Tripropylamine, Diethanolamine, Triethylamine, Triethanolamine;	
		Oleylamine (OA)/	[32]
		Ascorbic acid + OA;	
		Hydrogen peroxide	[36]
			[53]
		Ethyl acetate	
	Ethyl acetate/tetra-n-butylammonium hexafluorophosphate	Ethyl acetate + Tripropylamine	[52]
			[55]
	Dichloromethane/tetra-n-butylammonium hexafluorophosphate	Tripropylamine,	
		Benzoyl peroxide	[38]
	Acetonitrile	Tripropylamine	[56]
$CsPbBr_3$ (3D) Ce^{4+}-doped	Acetonitrile/tetra-n-butylammonium hexafluorophosphate	Tripropylamine	[27]
$CsPbBr_3$ (3D) Sb-doped	Acetonitrile/tetra-n-butylammonium hexafluorophosphate	Tripropylamine	[28]
$CsPbBr_3$ (3D) inside graphitic carbon nitride nanospheres	Phosphate-buffered solution	Ascorbic acid	[39]
$CsPbBr_3$ (3D)/aminated carbon dots in hierarchical zeolite imidazole framework-8	Phosphate-buffered solution	Tripropylamine	[33]

Table 1. *Cont.*

Type of Nanoparticles	Solution	Coreactant	References
$CsPbBr_3$ (3D)/N-doped graphene quantum dot	Phosphate-buffered solution	Amine groups of N-doped graphene quantum dot	[62]
$CsPbBr_3$ (3D) in SiO_2 shell	Dichloromethane/tetra-n-butylammonium hexafluorophosphate	2-(dibutylamino)ethanol, 2,2′-(butylimino)diethanol, 3-(diethylamino)propylamine, [3-(diethylamino)propyl] trimethoxysilane, Tripropylamine	[34]
$CsPbBr_3$ (3D)/ Ag^+ @UiO-66-NH2	Phosphate-buffered solution	Peroxydisulfate	[35]
$Rb_{0.2}Cs_{0.8}PbBr_3$ (3D)	Dichloromethane/tetra-n-butylammonium hexafluorophosphate	2-dibutyaminoethanol, Benzoyl peroxide	[54]
Cs_4PbBr_6 (0D)	Acetonitrile/tetra-n-butylammonium hexafluorophosphate	Benzoyl peroxide	[24]
$CH_3NH_3PbBr_3$ (3D)	Phosphate-buffered solution	Tripropylamine, Peroxydisulfate	[57]
$CH_3NH_3PbCl_{1.08}Br_{1.92}$ (3D)	Dichloromethane/tetra-n-butylammonium hexafluorophosphate	Tripropylamine	[40]
$Cs_3Bi_2Br_9$ (2D)	Acetonitrile/toluene/tetra-n-butylammonium hexafluorophosphate	Tripropylamine, Benzoyl peroxide	[25]
$CsPbCl_3$ Mn^{2+}-doped (3D)	Ethyl acetate	Benzoyl peroxide	[26]
$CH(NH_2)_2PbBr_3$ (3D)/ carbon nanotubes/TiO_2	Phosphate-buffered solution	Tripropylamine	[58]

Further subsections discuss more details about the mechanisms of anodic and cathodic ECL of PeNCs with coreactants and the potential for analytical application of such ECL systems.

6.1. Anodic ECL of Perovskite Nanocrystals

Several perovskite-like nanomaterials showed an anodic ECL behavior with the number of coreactants. The main challenge for anodic ECL is the interference of compounds in real samples that could be oxidized on the electrode at high positive potentials [31].

Most of the anodic ECL reactions have been conducted with classical all-inorganic PeNCs ($CsPbBr_3$). The following reagents were used as coreactants: ascorbic acid (on-set potential = 0.65 V; peak potential = 0.8 V) [30], hydrogen peroxide (peak potential = 1.2 V) [52], ethyl acetate (EA) (on-set potential = 0.85 V; peak potential = 0.95 V) [37], tripropylamine (on-set potential = 0.65 V; peak potential = 1.05 V) [32]. The scheme of the anodic ECL reaction of $CsPbBr_3$ PeNCs and TPrA, which is the most common anodic coreactant, is shown below:

$$CsPbBr_3 - e^- \rightarrow CsPbBr_3^{\bullet +} \quad (12)$$

$$TPrA - e^- \rightarrow TPrA^{\bullet +} \quad (13)$$

$$TPrA^{\bullet +} - H^+ \rightarrow TPrA^{\bullet} \quad (14)$$

$$CsPbBr_3^{\bullet +} + TPrA^{\bullet} \rightarrow CsPbBr_3^{*} + TPrA \text{ oxidate} \quad (15)$$

$$CsPbBr_3{}^* \rightarrow CsPbBr_3 + hv \quad (16)$$

Some groups investigated ECL of highly crystallized 3D organometallic halide PeNCs: $CH_3NH_3PbBr_3$ (on-set potential = 0.8 V and peak potential = 1.2 V) and $CH_3NH_3PbCl_{1.08}Br_{1.92}$ (on-set potential = 1.75 V and peak potential = 2.6 V) in aqueous medium with TPrA as coreactant [40,57]. Yue Cao et al. showed the ability of 2D all-inorganic lead-free PeNCs ($Cs_3Bi_2Br_9$) PeNCs to have ECL reactions with TPrA (on-set potential = 1.4 V; peak potential = 1,8 V) in the anodic potential range [25].

Besides TPrA, a group of other amine compounds was tested as anodic coreactants for PeNCs ECL generation [32]. The ECL intensity of $CsPbBr_3$ PeNCs increased as the coreactant was changed from diethylamine to triethylamine to tripropylamine. This is due to the ability of aliphatic alkyl groups to stabilize positive radical ions. As a result, an increase in the number and length of the alkyl chains attached to the nitrogen atom causes an increased ECL response. It was also demonstrated that the $CsPbBr_3$-triethanolamine system gave higher ECL than $CsPbBr_3$-triethylamine one even though both coreactants have the same number and length of alkyl chains. The reason is the catalysis of the electro-oxidation of amines by hydroxy groups leading to a substantial increase in ECL intensity.

Additionally, the possibility of enhancing of ECL signal of PeNCs by other nanomaterials was shown. Wang et al. achieved an ECL signal (on-set potential = 0.85 V; peak potential = 1.1 V) of 3D lead bromide PeNCs ($CH(NH_2)_2PbBr_3$) mixed with carbon nanotubes (CNTs) and deposited on a glassy carbon electrode with TPrA coreactant in phosphate-buffered solution. In this case, CNTs were also used as the electrical conductivity enhancer that reduces the impedance between PeNCs and glassy carbon electrodes. Such modification led to a lower impedance of the modified electrode which in turn increased the ECL intensity (Figure 7) [58].

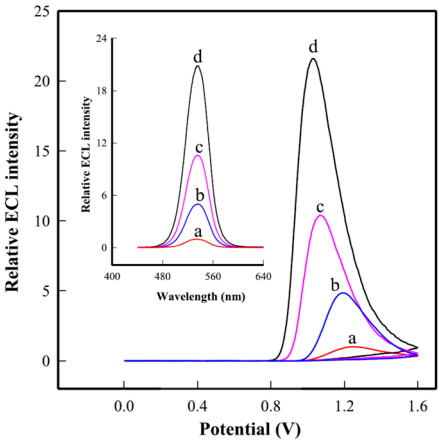

Figure 7. Anodic ECL profiles of $FAPbBr_3$ NC/GCE (a), TiO_2 NPs@$FAPbBr_3$ NC/GCE (b), $FAPbBr_3$ NC@CNT/GCE (c), and TiO_2 NP@$FAPbBr_3$ NC@CNTs/GCE (d) in pH 7.4 PBS containing 0.2 M KCl and 15 mM TPrA. Inset: oxidative-reduction ECL emission spectra. Reproduced with permission from Ref. [58]. © Elsevier.

Aside from ECL with coreactant in the solution comes the discovered self-enhanced ECL emission from $CsPbBr_3$ PeNCs with the surface oleylamine as both coreactant and stabilizer [36]. The ECL of $CsPbBr_3$ PeNCs was also observed in ethyl acetate media, and the solvent itself was claimed to act as a coreactant [52,55]. The system was used in a closed bipolar electrode configuration of the electrochemical cell as an indicator of redox processes taking place in a conjugated PBS-based redox system. The results suggested that ethyl acetate was undergoing oxidation at the electrode producing CH_3CO as one of the products. The latter serves as a reducer in the oxidative-reduction ECL pathway.

Therefore, a variety of PeNCs types and coreactants used for the generation of anodic ECL shows the great potential of such ECL systems to be used in existing analytical applications as a replacement for common fluorophores.

6.2. Cathodic ECL of Perovskite Nanocrystals

Cathodic ECL often offers such advantages as extending the number of possible ECL reactions, eliminating the oxidation products of luminophores, and removing the interference of compounds present in the samples that could be oxidized on the electrode at high positive potential [31,65].

All existing research of cathodic ECL with PeNCs has been conducted with structures that contain Cesium as A-site and Bromine as X-site, respectively. $CsPbBr_3$ PeNCs demonstrate cathodic ECL reaction with potassium peroxydisulfate ($K_2S_2O_8$) with on-set potential = −1.4 V and peak potential = −2.2 V. The scheme of this reaction is shown below [31]:

$$S_2O_8^{2-} + e \rightarrow SO_4^{2-} + SO_4^{\bullet} \quad (17)$$

$$SO_4^{\bullet} + CsPbBr_3 \rightarrow SO_4^{2-} + CsPbBr_3^{+} \quad (18)$$

$$CsPbBr_3 + e \rightarrow CsPbBr_3^{-} \quad (19)$$

$$CsPbBr_3^{+} + CsPbBr_3^{-} \rightarrow CsPbBr_3^{*} \quad (20)$$

$$CsPbBr_3^{*} \rightarrow CsPbBr_3 + hv \quad (21)$$

Rugeng Liu et al. achieved an ECL signal of 0D lead–halide PeNCs (Cs_4PbBr_6) with benzoyl peroxide as coreactant (on-set potential = −0.5 V and peak potential = −0.7 V) as shown in Figure 8 [24].

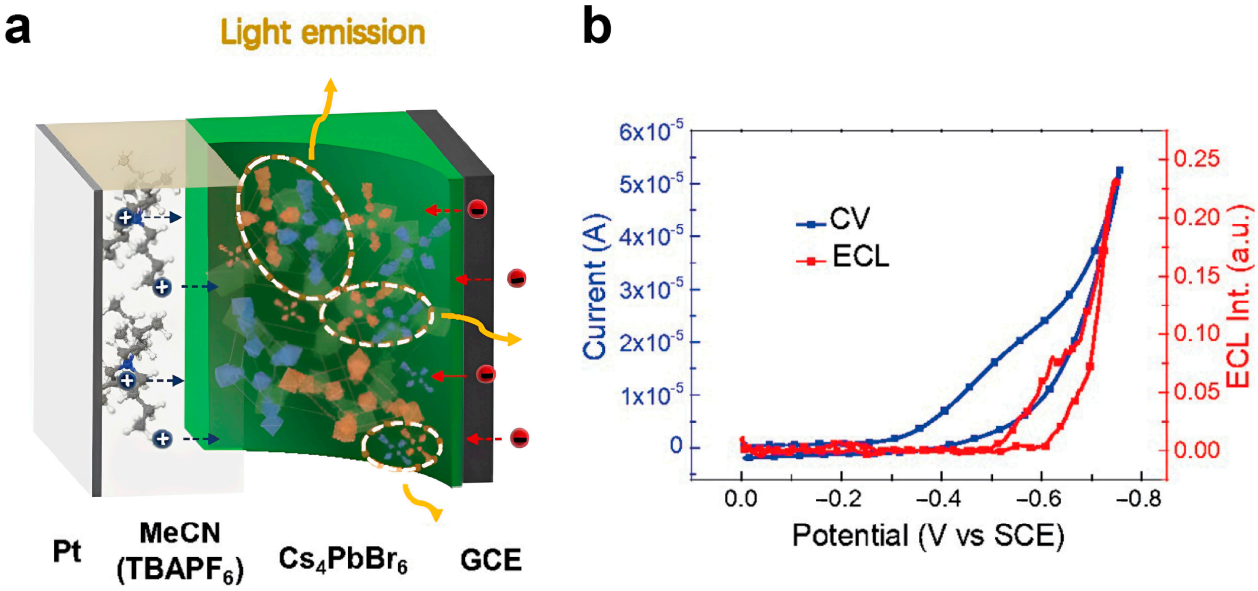

Figure 8. (**a**) Schematic drawing of Cs_4PbBr_6/GCE modified electrode and the light generation process therein. (**b**) ECL (Red curve)—CV (Blue curve) simultaneous measurements of Cs_4PbBr_6/GCE in the presence of 50 mM BPO as the coreactant by the pulsing potential from approximately 0.0 V to −0.75 V. Reproduced with permission from Ref. [24]. © Royal Society of Chemistry.

Cathodic ECL of $Cs_3Bi_2Br_9$ PeNCs with benzoyl peroxide coreactant (on-set potential = −1 V; peak potential = −1.2 V) was also studied by Yue Cao et al. alongside their anodic ECL with TPrA [25].

Despite examples of stable cathodic ECL emission of certain mentioned PeNCs, several works indicate much weaker ECL emission for the reductive-oxidation coreactant pathway [38,54,57]. The same tendency is confirmed by the radical ions annihilation pathway indicating that the ECL of PeNCs displays the "on/off" typed feature by changing the sequence of hole/electron injecting processes. Efficient ECL is often obtained by injecting holes into the electron-injected NPs while no or very weak ECL is obtained in the opposite case.

6.3. Analytical Application of ECL with Perovskite Nanocrystals

ECL of perovskite-related nanostructures is still quite a new area, but research conducted so far demonstrates numerous potential analytical applications. ECL at electrodes covered with PeNCs-containing films is used to detect and quantify numerous analytically important species in the solution by applying inhibition, coreaction, and impedance detection principles [36].

Among analytically important species that have coreactant properties and contribute to ECL generation with PeNCs are hydrogen peroxide [53,64] and ascorbic acid [36], which could be directly detected in the solution of PeNCs-modified electrodes.

Dopamine (an important neurotransmitter) has demonstrated efficient ECL quenching of the $CsPbBr_3$/TPrA system allowing its quantification in the 0.010–1.0 μM range with a detection limit of 0.0050 μM (S/N = 3) [64].

Hydrogen peroxide has also demonstrated the ability to quench ECL emission of the $CsPbBr_3$/oleylamine ECL system by scavenging intermediate radicals generated in the course of oleylamine oxidation [36]. The ECL system has demonstrated a 0.01–5 mM quantification range of hydrogen peroxide and a detection limit of 7.1 μM.

The detection of alkaline phosphatase enzyme was demonstrated with the detection limit of 0.714 mU/L due to its ability to convert ascorbic acid 2-phosphate to ascorbic acid which in turn serves as ECL coreactant for $CsPbBr_3$ PeNCs [30].

The impedance detection principle of HeLa cells became possible because of the high impedance of cells. The $CsPbBr_3$/oleylamine ECL system was inhibited due to electrode surface blockage. The PeNCs-covered electrode was further bio-functionalized with folic acid in a mixture with chitosan solution to capture HeLa cells. The constructed label-free signal-off biosensor was sensing HeLa cells from 0.5 to 15 Kcells mL^{-1} and had a detection limit of 0.24 Kcells mL^{-1} [36].

A ratiometric ECL quantification of CD44 receptors expression on the MCF-7 cell surface and MCF-7 cells concentration can be made by simultaneously recording anodic and cathodic ECL from nanocomposite made of $CsPbBr_3$ PeNCs inside of hollow graphitic carbon nitride nanospheres [39]. The anodic ECL originating from PeNCs in the presence of ascorbic acid coreactant is quenched due to resonant energy transfer onto rhodamine 6G labels on the MCF-7 cell surface whereas cathodic ECL from graphitic carbon nitride nanospheres in reaction with dissolved oxygen remains unchanged, thus serving as an internal standard for a ratiometric analysis. The sensing strategy exhibited good analytical performance for MCF-7 cells, ranging from 1.0 × 103 to 3.2 × 105 cells mL^{-1} with a detection limit of 320 cells mL^{-1}.

Prometryn, a selective internal absorption-conducting triazine herbicide that is banned in many countries because of its endocrine-disrupting property and potential environmental and health risks, was successfully detected using an MIP-based PeNC ECL sensor. Prometryn was blocking cavities of MIP film, thus hindering electron transfer and quenching the $CsPbBr_3/H_2O_2$ ECL system, which allowed its detection in the range of 0.10–500.0 μg/L [63]. The technique was shown applicable for prometryn detection in fish and seawater samples.

Another analyte that was successfully detected using an MIP-based PeNC ECL sensor is nitrofurazone—a synthetic nitrofuran derivative with an antibacterial effect [35]. Nitrofurazone has exhibited the properties of the co-reaction promoter in the $CsPbBr_3/S_2O_8^{2-}$ ECL system, and the ECL signal was linearly proportional to its concentration in the range of 0.5–100 μM.

Ochratoxin A detection with an MIP-based PeNC ECL sensor was based on the blockage of MIP cavities by the analyte and corresponding reduction in ECL response of self-enhanced superstructures of N-doped graphene quantum dots and $CsPbBr_3$ PeNCs on graphene supported two-dimensional mesoporous SiO_2 nanosheets [62]. The ECL sensor has demonstrated the linear range from 10^{-5} ng/mL to 1.0 ng/mL.

Separately, it is worth mentioning the closed bipolar electrode system approach, where the ECL reaction of PeNCs modified electrode in organic solvent on one end of a bipolar

electrode is used to report redox reaction taking place on the other end of the electrode in aqueous solution. Using this approach, it was possible to quantify hydrogen peroxide [52] and tetracycline (a broad-spectrum antibiotic) on an aptamer-modified electrode [55].

7. Conclusions

The conducted review of recent scientific works reveals perspectives and possibilities of application of perovskite and perovskite-related nanocrystals as light emitters for the generation of electrochemiluminescence with coreactants and development of corresponding analytical techniques.

The list of research aimed at ECL detection of various analytes (coreactants) with the use of PeNCs has been systematized. It was found that despite a relatively small number of publications, they cover various classes of analytes including such common small molecular substances of biological significance as hydrogen peroxide, ascorbic acid, and dopamine as well as more complicated biological species such as enzymes (alkaline phosphatase) and even whole cells (HeLa cells), and also examples of herbicides (prometryn) and synthetic antibacterial substances (nitrofurazone).

Additionally, the possibility of the use of PeNCs, synthesized by hot-injection and LARP techniques, in aqueous and non-aqueous solutions as well as in the cathodic and anodic range of potentials for the generation of ECL emission has been shown. The vast majority of reviewed PeNCs used for ECL generation were either pristine $CsPbBr_3$ 3D perovskite structures or nanocomposite containing $CsPbBr_3$ moiety linked with some other nanostructures (carbon or graphene quantum dots) or within a shell (SiO_2, carbon nitride nanospheres)/metal-organic framework. Other scarce examples include 3D perovskite structures of CsPbBr3 doped with some ions (Ce^{4+}; Sb^{3+}), 2D perovskite structures of $Rb_{0.2}Cs_{0.8}PbBr_3$ and $Cs_3Bi_2Br_9$, the 0D structure of Cs_4PbBr_6 as well as 3D structures of organic-inorganic perovskites $CH_3NH_3PbBr_3$, $CH_3NH_3PbCl_{1.08}Br_{1.92}$, and $CH(NH_2)_2PbBr_3$.

Various types of coreactants used for ECL generation mostly belong to oxidative-reduction types such as ascorbic acid, various amines such as tripropylamine and 2-(dibutylamino)ethanol, and some other less commonly applicable members of this class, such as ethyl acetate (used as reaction media). Only a few works were dealing with the reductive oxidation type of ECL coreactant such as peroxydisulfate and benzoyl peroxide, and in several cases, these ECL systems were demonstrating poor ECL efficiency.

The great potential of the use of this class of nanomaterials in the ECL method of analysis of liquids has been illustrated. Existing analytical applications of PeNCs-based ECL systems demonstrate the feasibility of exploiting almost all available ECL detection principles including ECL inhibition, coreaction, ratiometric analysis, and altering electrode impedance. It is worth noting that all analytical applications are based on ECL from PeNCs immobilized in a form of a thin film on the electrode surface.

Despite a variety of successful and promising examples of applications, research on perovskite ECL systems is still in its infancy, and further systematic study of the ability to detect different classes of analytes and elucidate the ECL mechanisms involved is needed. Here, it should be noted that the majority of discussed works only propose some non-contradictory hypotheses about the mechanisms of ECL generation, and much deeper and more dedicated research is necessary to prove their validity.

Further work should also focus on PeNCs stability in electrochemical experiments with an emphasis on the optimization of PeNCs structure and synthesis techniques providing such stability.

The design of a new efficient ECL system with PeNCs should pay special attention to the choice of suitable coreactant that meets the required potential range and chemistry of analytical reaction, the proper type of PeNCs capable of ECL emission under required conditions, and approaches providing stability of selected PeNCs within the selected ECL system.

Author Contributions: Conceptualization, V.V., I.B., Y.Z.; writing—original draft preparation, V.V., I.B., Y.Z.; writing—review and editing, M.S., B.C.; supervision, M.S., B.C.; project administration, M.S., O.S., B.C.; funding acquisition, B.C. All authors have read and agreed to the published version of the manuscript.

Funding: This work was funded by the Federal Ministry of Education and Research of Germany project "Funding of the German-Ukrainian Cores of Excellence" (grant number: 01DK21007) and the National Research Foundation of Ukraine (grant number: 2020.02/0390).

Data Availability Statement: Publicly available datasets were analyzed in this study.

Conflicts of Interest: The authors declare no conflict of interest.

References

1. Pyati, R.; Richter, M.M. ECL—Electrochemical luminescence. *Annu. Rep. Prog. Chem. Sect. C Phys. Chem.* **2007**, *103*, 12–78. [CrossRef]
2. Hesari, M.; Ding, Z. Review—Electrogenerated Chemiluminescence: Light Years Ahead. *J. Electrochem. Soc.* **2015**, *163*, H3116–H3131. [CrossRef]
3. Miao, W. Electrogenerated Chemiluminescence and Its Biorelated Applications. *Chem. Rev.* **2008**, *108*, 2506–2553. [CrossRef] [PubMed]
4. Zhang, R.; Ding, Z. Electrochemiluminescence Biochemical Sensors. *Biochem. Sens.* **2021**, 125–212. [CrossRef]
5. Majeed, S.; Gao, W.; Zholudov, Y.; Muzyka, K.; Xu, G. Electrochemiluminescence of Acridines. *Electroanalysis* **2016**, *28*, 2672–2679. [CrossRef]
6. Sun, J.; Sun, H.; Liang, Z. Nanomaterials in Electrochemiluminescence Sensors. *ChemElectroChem* **2017**, *4*, 1651–1662. [CrossRef]
7. Yuan, Y.; Li, J.; Xu, G. Chapter 4. Electrochemiluminescence Coreactants. *Detect. Sci.* **2019**, 92–133. [CrossRef]
8. Zanut, A.; Fiorani, A.; Canola, S.; Saito, T.; Ziebart, N.; Rapino, S.; Rebeccani, S.; Barbon, A.; Irie, T.; Josel, H.-P.; et al. Insights into the mechanism of coreactant electrochemiluminescence facilitating enhanced bioanalytical performance. *Nat. Commun.* **2020**, *11*, 2668. [CrossRef]
9. Zholudov, Y.T.; Lysak, N.; Snizhko, D.V.; Reshetniak, O.; Xu, G. Electrochemiluminescence analysis of tryptophan in aqueous solutions based on its reaction with tetraphenylborate anions. *Analyst* **2020**, *145*, 3364–3369. [CrossRef]
10. Cumba, L.; Pellegrin, Y.; Melinato, F.; Forster, R.J. Enhanced Electrochemiluminescence from 3D Nanocavity Electrode Arrays. *Sens. Actuators Rep.* **2022**, *4*, 100082. [CrossRef]
11. Valenti, G.; Fiorani, A.; Li, H.; Sojic, N.; Paolucci, F. Essential Role of Electrode Materials in Electrochemiluminescence Applications. *ChemElectroChem* **2016**, *3*, 1990–1997. [CrossRef]
12. Gao, W.; Muzyka, K.; Ma, X.; Lou, B.; Xu, G. A single-electrode electrochemical system for multiplex electrochemiluminescence analysis based on a resistance induced potential difference. *Chem. Sci.* **2018**, *9*, 3911–3916. [CrossRef]
13. Bouffier, L.; Arbault, S.; Kuhn, A.; Sojic, N. Generation of electrochemiluminescence at bipolar electrodes: Concepts and applications. *Anal. Bioanal. Chem.* **2016**, *408*, 7003–7011. [CrossRef] [PubMed]
14. Muzyka, K.; Saqib, M.; Liu, Z.; Zhang, W.; Xu, G. Progress and challenges in electrochemiluminescent aptasensors. *Biosens. Bioelectron.* **2017**, *92*, 241–258. [CrossRef] [PubMed]
15. Rizwan, M.; Mohd-Naim, N.F.; Ahmed, M.U. Trends and Advances in Electrochemiluminescence Nanobiosensors. *Sensors* **2018**, *18*, 166. [CrossRef]
16. Hazelton, S.G.; Zheng, X.; Zhao, J.X.; Pierce, D.T. Pierce, Developments and Applications of Electrogenerated Chemiluminescence Sensors Based on Micro- and Nanomaterials. *Sensors* **2008**, *8*, 5942–5960. [CrossRef]
17. Zanut, A.; Palomba, F.; Scota, M.R.; Rebeccani, S.; Marcaccio, M.; Genovese, D.; Rampazzo, E.; Valenti, G.; Paolucci, F.; Prodi, L. Dye-Doped Silica Nanoparticles for Enhanced ECL-Based Immunoassay Analytical Performance. *Angew. Chem.* **2020**, *132*, 22042–22047. [CrossRef]
18. Huang, H. *Synthesis of Perovskite Nanocrystals*; Springer Series in Materials Science; Springer: Berlin, Germany, 2020; pp. 1–18. [CrossRef]
19. Chouhan, L.; Ghimire, S.; Subrahmanyam, C.; Miyasaka, T.; Biju, V. Synthesis, optoelectronic properties and applications of halide perovskites. *Chem. Soc. Rev.* **2020**, *49*, 2869–2885. [CrossRef]
20. Zang, Z.; Yan, D. All-inorganic perovskite quantum dots: Ligand modification, surface treatment and other strategies for enhanced stability and durability. In *Perovskite Quantum Dots*; Springer Series in Materials Science; Springer: Berlin, Germany, 2020; pp. 51–106. [CrossRef]
21. Bartel, C.J.; Sutton, C.; Goldsmith, B.R.; Ouyang, R.; Musgrave, C.B.; Ghiringhelli, L.M.; Scheffler, M. New tolerance factor to predict the stability of perovskite oxides and halides. *Sci. Adv.* **2019**, *5*, eaav0693. [CrossRef]
22. Dai, T.; Cao, Q.; Yang, L.; Aldamasy, M.; Li, M.; Liang, Q.; Lu, H.; Dong, Y.; Yang, Y. Strategies for High-Performance Large-Area Perovskite Solar Cells toward Commercialization. *Crystals* **2021**, *11*, 295. [CrossRef]
23. Shamsi, J.; Urban, A.S.; Imran, M.; De Trizio, L.; Manna, L. Metal Halide Perovskite Nanocrystals: Synthesis, Post-Synthesis Modifications, Their Optical Properties. *Chem. Rev.* **2019**, *119*, 3296–3348. [CrossRef] [PubMed]

24. Liu, R.; Mak, C.H.; Han, X.; Tang, Y.; Jia, G.; Cheng, K.-C.; Qi, H.; Zou, X.; Zou, G.; Hsu, H.-Y. Efficient electronic coupling and heterogeneous charge transport of zero-dimensional Cs_4PbBr_6 perovskite emitters. *J. Mater. Chem. A* **2020**, *8*, 23803–23811. [CrossRef]
25. Cao, Y.; Zhang, Z.; Li, L.; Zhang, J.-R.; Zhu, J.-J. An Improved Strategy for High-Quality Cesium Bismuth Bromine Perovskite Quantum Dots with Remarkable Electrochemiluminescence Activities. *Anal. Chem.* **2019**, *91*, 8607–8614. [CrossRef] [PubMed]
26. Bai, X.; Zhong, H.; Chen, B.; Chen, C.; Han, J.; Zeng, R.; Zou, B. Discovering the Link between Electrochemiluminescence and Energy Transfer Pathways for Mn-Doped $CsPbCl_3$ Quantum Dot Films. *J. Phys. Chem. C* **2018**, *122*, 3130–3137. [CrossRef]
27. Fu, L.; Fu, K.; Hsu, H.-Y.; Gao, X.; Zou, G. Ce4+ doping to modulate electrochemical and radiative-charge-transfer behaviors of $CsPbBr_3$ perovskite nanocrystals. *J. Electroanal. Chem.* **2020**, *876*, 114546. [CrossRef]
28. Jia, J.; Fu, K.; Hou, S.; Zhang, B.; Fu, L.; Hsu, H.-Y.; Zou, G. Enhanced Charge Injection and Recombination of $CsPbBr_3$ Perovskite Nanocrystals upon Internal Heterovalent Substitution. *J. Phys. Chem. C* **2019**, *123*, 29916–29921. [CrossRef]
29. State of the Art and Prospects for Halide Perovskite Nanocrystals. *ACS Nano* **2021**, *15*, 10775–10981. [CrossRef] [PubMed]
30. Wang, X.-Y.; Wu, M.-X.; Ding, S.-N. Anodic electrochemiluminescence from $CsPbBr_3$ perovskite quantum dots for an alkaline phosphatase assay. *Chem. Commun.* **2020**, *56*, 8099–8102. [CrossRef]
31. Peng, H.; Wu, W.; Huang, Z.; Xu, L.; Sheng, Y.; Deng, H.; Xia, X.; Chen, W. Cathodic electrochemiluminescence performance of all-inorganic perovskite $CsPbBr_3$ nanocrystals in an aqueous medium. *Electrochem. Commun.* **2020**, *111*, 106667. [CrossRef]
32. Cai, Z.; Li, F.; Xu, W.; Xia, S.; Zeng, J.; He, S.; Chen, X. Colloidal $CsPbBr_3$ perovskite nanocrystal films as electrochemiluminescence emitters in aqueous solutions. *Nano Res.* **2018**, *11*, 1447–1455. [CrossRef]
33. Cao, Y.; Zhou, Y.; Lin, Y.; Zhu, J.-J. Hierarchical Metal–Organic Framework-Confined $CsPbBr_3$ Quantum Dots and Aminated Carbon Dots: A New Self-Sustaining Suprastructure for Electrochemiluminescence Bioanalysis. *Anal. Chem.* **2020**, *93*, 1818–1825. [CrossRef]
34. Li, L.; Zhang, Z.; Chen, Y.; Xu, Q.; Zhang, J.; Chen, Z.; Chen, Y.; Zhu, J. Sustainable and Self-Enhanced Electrochemiluminescent Ternary Suprastructures Derived from $CsPbBr_3$ Perovskite Quantum Dots. *Adv. Funct. Mater.* **2019**, *29*, 1902533. [CrossRef]
35. Liu, T.; He, J.; Lu, Z.; Sun, M.; Wu, M.; Wang, X.; Jiang, Y.; Zou, P.; Rao, H.; Wang, Y. A visual electrochemiluminescence molecularly imprinted sensor with Ag^+@UiO-66-NH_2 decorated $CsPbBr_3$ perovskite based on smartphone for point-of-care detection of nitrofurazone. *Chem. Eng. J.* **2022**, *429*, 132462. [CrossRef]
36. Cao, Y.; Zhu, W.; Li, L.; Zhang, Z.; Chen, Z.; Lin, Y.; Zhu, J.-J. Size-selected and surface-passivated $CsPbBr_3$ perovskite nanocrystals for self-enhanced electrochemiluminescence in aqueous media. *Nanoscale* **2020**, *12*, 7321–7329. [CrossRef]
37. Xue, J.; Zhang, Z.; Zheng, F.; Xu, Q.; Xu, J.; Zou, G.; Li, L.; Zhu, J.-J. Efficient Solid-State Electrochemiluminescence from High-Quality Perovskite Quantum Dot Films. *Anal. Chem.* **2017**, *89*, 8212–8216. [CrossRef] [PubMed]
38. Huang, Y.; Fang, M.; Zou, G.; Zhang, B.; Wang, H. Monochromatic and electrochemically switchable electrochemiluminescence of perovskite $CsPbBr_3$ nanocrystals. *Nanoscale* **2016**, *8*, 18734–18739. [CrossRef] [PubMed]
39. Cao, Y.; Zhu, W.; Wei, H.; Ma, C.; Lin, Y.; Zhu, J.-J. Stable and Monochromatic All-Inorganic Halide Perovskite Assisted by Hollow Carbon Nitride Nanosphere for Ratiometric Electrochemiluminescence Bioanalysis. *Anal. Chem.* **2020**, *92*, 4123–4130. [CrossRef]
40. Wusimanjiang, Y.; Yadav, J.; Arau, V.; Steen, A.E.; Hammer, N.I.; Pan, S. Blue Electrogenerated Chemiluminescence from Halide Perovskite Nanocrystals. *J. Anal. Test.* **2019**, *3*, 125–133. [CrossRef]
41. Tang, Y.; Yan, N.; Wang, Z.; Yuan, H.; Xin, Y.; Yin, H. Precursor solution volume-dependent ligand-assisted synthesis of $CH_3NH_3PbBr_3$ perovskite nanocrystals. *J. Alloy. Compd.* **2019**, *773*, 227–233. [CrossRef]
42. Hu, X.; Xu, Y.; Wang, J.; Ma, J.; Wang, L.; Jiang, W. Scalable synthesis of efficiently luminescent and color-tunable $CsPbX_3$ (X=Cl, Br, I) nanocrystals by regulating the reaction parameters. *J. Lumin.* **2022**, *251*, 119191. [CrossRef]
43. Soosaimanickam, A.; Rodríguez-Cantó, P.J.; Martínez-Pastor, J.P.; Abargues, R. Chapter 6 -Recent advances in synthesis, surface chemistry of cesium lead-free halide perovskite nanocrystals and their potential applications. *Nanostructured Funct. Flex. Mater. Energy Convers. Storage Syst.* **2020**, 157–228. [CrossRef]
44. Ma, H.H.; Imran, M.; Dang, Z.; Hu, Z. Growth of Metal Halide Perovskite, from Nanocrystal to Micron-Scale Crystal: A Review. *Crystals* **2018**, *8*, 182. [CrossRef]
45. Yang, G. Laser ablation in liquids: Applications in the synthesis of nanocrystals. *Prog. Mater. Sci.* **2007**, *52*, 648–698. [CrossRef]
46. Semaltianos, N.G. Nanoparticles by Laser Ablation. *Crit. Rev. Solid State Mater. Sci.* **2010**, *35*, 105–124. [CrossRef]
47. Hahn, A. Influences on Nanoparticle Production during Pulsed Laser Ablation. *J. Laser Micro/Nanoeng.* **2008**, *3*, 73–77. [CrossRef]
48. Kanaujia, P.K.; Prakash, G.V. Laser-induced microstructuring of two-dimensional layered inorganic–organic perovskites. *Phys. Chem. Chem. Phys.* **2016**, *18*, 9666–9672. [CrossRef]
49. Zoski, C.G. *Handbook of Electrochemistry*; Elsevier: Amsterdam, The Netherlands, 2007; pp. v–vi. [CrossRef]
50. Bertoncello, P.; Ugo, P. Recent Advances in Electrochemiluminescence with Quantum Dots and Arrays of Nanoelectrodes. *ChemElectroChem* **2017**, *4*, 1663–1676. [CrossRef]
51. Vasylkovskyi, V.S.; Slipchenko, M.I.; Slipchenko, O.V.; Muzyka, K.M.; Zholudov, Y.T. Laser-induced nanoparticles in electroanalysis: Review. *Funct. Mater.* **2021**, *28*, 210–2016. [CrossRef]
52. Hao, N.; Lu, J.; Dai, Z.; Qian, J.; Zhang, J.; Guo, Y.; Wang, K. Analysis of aqueous systems using all-inorganic perovskite CsPbBr3 quantum dots with stable electrochemiluminescence performance using a closed bipolar electrode. *Electrochem. Commun.* **2019**, *108*, 106559. [CrossRef]

53. Huang, Y.; Long, X.; Shen, D.; Zou, G.; Zhang, B.; Wang, H. Hydrogen Peroxide Involved Anodic Charge Transfer and Electrochemiluminescence of All-Inorganic Halide Perovskite CsPbBr3 Nanocrystals in an Aqueous Medium. *Inorg. Chem.* **2017**, *56*, 10135–10138. [CrossRef]
54. Chen, L.; Kang, Q.; Li, Z.; Zhang, B.; Zou, G.; Shen, D. Tunable electrochemiluminescence properties of $CsPbBr_3$ perovskite nanocrystals using mixed-monovalent cations. *New J. Chem.* **2020**, *44*, 3323–3329. [CrossRef]
55. Hao, N.; Qiu, Y.; Lu, J.; Han, X.; Li, Y.; Qian, J.; Wang, K. Flexibly regulated electrochemiluminescence of all-inorganic perovskite $CsPbBr_3$ quantum dots through electron bridge to across interfaces between polar and non-polar solvents. *Chin. Chem. Lett.* **2021**, *32*, 2861–2864. [CrossRef]
56. Qiu, L.; Lin, L.; Huang, Y.; Lai, Z.; Li, F.; Wang, S.; Lin, F.; Li, J.; Wang, Y.; Chen, X. Unveiling the interfacial electrochemiluminescence behavior of lead halide perovskite nanocrystals. *Nanoscale Adv.* **2019**, *1*, 3957–3962. [CrossRef]
57. Tan, X.; Zhang, B.; Zou, G. Electrochemistry and Electrochemiluminescence of Organometal Halide Perovskite Nanocrystals in Aqueous Medium. *J. Am. Chem. Soc.* **2017**, *139*, 8772–8776. [CrossRef]
58. Wang, X.; Yu, L.; Kang, Q.; Chen, L.; Jin, Y.; Zou, G.; Shen, D. Enhancing electrochemiluminescence of FAPbBr3 nanocrystals by using carbon nanotubes and TiO_2 nanoparticles as conductivity and co-reaction accelerator for dopamine determination. *Electrochim. Acta* **2020**, *360*, 136992. [CrossRef]
59. Kumar, A.K.S.; Zhang, Y.; Li, D.; Compton, R.G. Compton, A mini-review: How reliable is the drop casting technique? *Electrochem. Commun.* **2020**, *121*, 106867. [CrossRef]
60. Sahu, N.; Parija, B.; Panigrahi, S. Fundamental understanding and modeling of spin coating process: A review. *Indian J. Phys.* **2009**, *83*, 493–502. [CrossRef]
61. Gao, T.; Jessem, B.P. Nanoelectrochromics for Smart Windows: Materials and Methodologies, Materials for Energy. *Effic. Sustain. TechConnect Briefs* **2016**, *2*, 279–282.
62. Wei, J.; Chen, L.; Cai, X.; Lai, W.; Chen, X.; Cai, Z. 2D mesoporous silica-confined $CsPbBr_3$ nanocrystals and N-doped graphene quantum dot: A self-enhanced quaternary composite structures for electrochemiluminescence analysis. *Biosens. Bioelectron.* **2022**, *216*, 114664. [CrossRef] [PubMed]
63. Zhang, R.-R.; Gan, X.-T.; Xu, J.-J.; Pan, Q.-F.; Liu, H.; Sun, A.-L.; Shi, X.-Z.; Zhang, Z.-M. Ultrasensitive electrochemiluminescence sensor based on perovskite quantum dots coated with molecularly imprinted polymer for prometryn determination. *Food Chem.* **2022**, *370*, 131353. [CrossRef]
64. Wang, Y.; Chen, T.; Huang, C.; Wang, Y.; Wu, J.; Sun, B. Electrochemically switchable electrochemiluminescent sensor constructed based on inorganic perovskite quantum dots synthesized with microwave irradiation *J. Electroanal. Chem.* **2020**, *867*, 114181. [CrossRef]
65. Ballesta-Claver, J.; Rodríguez-Gómez, R.; Capitán-Vallvey, L. Disposable biosensor based on cathodic electrochemiluminescence of tris(2,2-bipyridine)ruthenium(II) for uric acid determination. *Anal. Chim. Acta* **2013**, *770*, 153–160. [CrossRef] [PubMed]